Ab Initio Structure of *p*-Shell Nuclei with Chiral Effective Field Theory and Daejeon16 Interactions

Pieter Maris[a], Ik Jae Shin[b], and James P. Vary[a]

[a] *Department of Physics and Astronomy, Iowa State University, Ames, IA 50011, USA*
[b] *Rare Isotope Science Project, Institute for Basic Science, Daejeon 34047, Korea*

Abstract

We present No-Core Full Configuration results for the ground state energies of all particle-stable *p*-shell nuclei, as well as the excitation energies of more than 40 narrow states, excluding isobaric analog states. We used the chiral LENPIC nucleon-nucleon plus three-nucleon interaction at N^2LO with semi-local coordinate space regulators, and also the phenomenological Daejeon16 nucleon-nucleon potential. With simple exponential extrapolations of the total energies of each state, binding energies and spectra are found to be in good agreement with experiment. Both interactions produce a trend towards some overbinding of nuclei at the upper end of the *p*-shell.

Keywords: *Ab initio nuclear structure; binding energies; spectra*

1 Introduction

Recent advances in models of the strong internucleon interactions and in many-body methods to solve, with high precision, the properties of light nuclei have opened new frontiers of fundamental research opportunities. Extensive efforts are underway to continue improving the effective interactions between nucleons based on the strong interactions of QCD and to incorporate improved electroweak operators to better understand the physics of the standard model in a data rich domain. These efforts are also building a foundation for searching for new laws of physics that may be revealed, for example, in experiments seeking to measure neutrinoless double-beta decay. We report here on results for light nuclei that, with their quantified uncertainties, indicate that highly accurate descriptions of the spectroscopy of light nuclei, which provide good agreement with experiment, are becoming available.

We follow an established approach to solve the non-relativistic quantum many-body problem of the structure of light nuclei with realistic strong interactions. The method we adopt is called the No-Core Full Configuration (NCFC) approach [1] that is based on the No-Core Shell Model (NCSM) [2, 3] with the improvement of extrapolating finite-basis results to the continuum limit. Both the NCSM and the NCFC

Proceedings of the International Conference 'Nuclear Theory in the Supercomputing Era — 2018' (NTSE-2018), Daejeon, South Korea, October 29 – November 2, 2018, eds. A. M. Shirokov and A. I. Mazur. Pacific National University, Khabarovsk, Russia, 2019, p. 168.

http://www.ntse.khb.ru/files/uploads/2018/proceedings/Vary.pdf.

belong to a class of approaches grouped under No-Core Configuration Interaction (NCCI) methods.

For our internucleon interactions, we select two recently developed models. On the one hand, we select the Low Energy Nuclear Physics International Collaboration (LENPIC) [4] nucleon-nucleon (NN) plus three-nucleon ($3N$) interactions developed within the framework of chiral effect field theory (χEFT) [5] through Next-to-Next-to Leading Order (N^{2}LO) [6–9]. These interactions were recently shown to produce good $3N$ scattering properties as well as good binding energies of light nuclei [10–12]. On the other hand, we adopt the Daejeon16 NN interaction [13] which is developed from a χEFT approach through Next-to-Next-to-Next-to Leading Order (N^{3}LO) [14–16] followed by additional two-body unitary phase-equivalent transformations (PET) [17–20] to reduce its high momentum components and to adjust its off-shell properties to provide good descriptions of selected properties of light nuclei [13].

Our goal here is to compare NCFC results of these two internucleon interactions with each other and with experiment. We focus on the energies of the ground and narrow excited states of the p-shell nuclei, including states of both parities. Our NCFC results show that, within our extrapolation uncertainties, both internucleon interactions provide good descriptions of the energies of these light nuclei with a noticeable tendency to overbind nuclei at the upper end of the p-shell. Some of the LENPIC results presented here have appeared in Refs. [12, 21].

2 *Ab initio* nuclear structure calculations

A successful theory of atomic nuclei involves two major challenges. The first is to accurately define the internucleon interactions so that results for NN, $3N$ and $4N$ systems, which can be solved to high accuracy, are in good agreement with experimental data. The second is to develop accurate computational many-body methods to enable calculations of properties of nuclei with atomic number $A \geq 5$. We report here on particular combinations of these two elements that provide encouraging results for light nuclei. We begin with a brief description of the NCFC approach.

2.1 No-Core Full Configuration approach

In non-relativistic quantum mechanics, we define the dynamics through the many-body Hamiltonian which consists of sums over the relative kinetic energy between pairs of nucleons, the pairwise interactions, three-body interactions, etc., as

$$\hat{\mathbf{H}} = \sum_{i<j} \frac{(\vec{p}_i - \vec{p}_j)^2}{2\, m\, A} + \sum_{i<j} V_{ij} + \sum_{i<j<k} V_{ijk} + ... \tag{1}$$

where m is the nucleon mass taken here to be equal for protons and neutrons. We then seek the solutions of the many-body eigenvalue equation

$$\hat{\mathbf{H}}\, \Psi(\vec{r}_1, \dots, \vec{r}_A) = E\, \Psi(\vec{r}_1, \dots, \vec{r}_A) \tag{2}$$

which yields the eigenenergies E and the wave functions Ψ for each state.

In the NCCI nuclear structure calculations, the wave function Ψ of a nucleus is expanded in an A-body basis of Slater determinants Φ_k of single-particle wave functions $\phi_{nljm}(\vec{r})$. Here, n (l) is the radial (orbital) quantum number, j is the total angular momentum resulting from orbital motion coupled to the intrinsic nucleon spin, and m is the projection of the total angular momentum on the z-axis, the axis of quantization. We construct the Slater determinant basis from separate Slater determinants for the neutrons and the protons in order to retain charge dependence in the basis.

The Hamiltonian $\hat{\mathbf{H}}$ is then evaluated in this Slater determinant basis which results in a Hamiltonian matrix eigenvalue problem. Beyond $A = 4$ with NN plus $3N$ interactions, the Hamiltonian matrix becomes increasingly sparse as A grows and/or the basis dimension increases. Upon diagonalization, the resulting eigenvalues can be compared with the experimental total binding energies of nuclear states. The resulting wave functions are then employed to evaluate additional observables for comparison with experiments. Electromagnetic moments and transitions, along with weak decays, are among the popular applications of these wave functions.

Following our common practice, we adopt a harmonic oscillator (HO) basis with energy parameter $\hbar\omega$ for the single-particle wave functions. We truncate the complete (infinite-dimensional) basis with a cutoff in the total number of HO quanta: the basis is limited to Slater determinants with $\sum_A N_i \leq N_0 + N_{\max}$, with N_0 the minimal number of quanta for that nucleus (the sum over the HO single-particle quanta $2n+l$ of the occupied orbitals) and $N_{\max}$ the truncation parameter. Even (odd) values of $N_{\max}$ provide results for natural (unnatural) parity. Numerical convergence toward the exact results for a given Hamiltonian is obtained with increasing $N_{\max}$, and is marked by approximate $N_{\max}$ and $\hbar\omega$ independence. In the NCFC approach we use extrapolations to estimate the binding energy in the complete (infinite-dimensional) space based on a sequence of calculations in finite bases [1, 22–27].

Here, we solve for the eigenvalues of a given nucleus in a sequence of basis spaces defined by the cutoff $N_{\max}$ and as a function of $\hbar\omega$. Subsequently, we use a simple three-parameter exponential form to extrapolate results at a sequence of three $N_{\max}$ values at fixed $\hbar\omega$

$$E(N_{\max}) \approx E_\infty + a \exp\left(-b N_{\max}\right) \tag{3}$$

around the variational minimum in $\hbar\omega$. We employ the sensitivity of the extrapolant to the highest $N_{\max}$ value and its sensitivity to $\hbar\omega$ to estimate the extrapolation uncertainty for each state's energy, as detailed below where we present our results.

The rate of convergence depends both on the nucleus and on the interaction. For typical realistic interactions, the dimension of the matrix needed to reach a sufficient level of convergence is in the billions, and the number of nonzero matrix elements is in the tens of trillions, which saturates available storage on current High-Performance Computing facilities. All NCFC calculations presented here were performed on the Cray XC30 Edison and Cray XC40 Cori at NERSC and the IBM BG/Q Mira at Argonne National Laboratory, using the code MFDn [28, 29].

2.2 Chiral EFT $NN + 3N$ interaction

The χEFT allows us to derive internucleon interactions (and the corresponding electroweak current operators) in a systematic way [5–9, 14–16]. The χEFT expansion is not unique: e. g., different choices for the degrees of freedom, such as whether or not to include Δ isobars explicitly, lead to different χEFT interactions. In addition, there is freedom to choose the functional form of regulators.

We adopt the χEFT interactions of the LENPIC collaboration [10–12] which have been developed to describe NN and nucleon-deuteron scattering and have been applied to the structure of light-mass and medium-mass nuclei. Specifically, we adopt the semi-local coordinate-space regularized χEFT potentials of Refs. [8, 9]. The Leading Order (LO) and Next-to-Leading Order (NLO) contributions are given by NN-only potentials while $3N$ interactions appear first at N^2LO in the χEFT expansion [6, 7, 16]. Four-nucleon forces are even more suppressed and start contributing at N^3LO. The χEFT power counting thus provides a natural explanation of the observed hierarchy of nuclear forces.

The Low-Energy Constants (LECs) in the NN-only potentials of Refs. [8, 9] have been fitted to NN scattering data, without any input from nuclei with $A > 2$. The $3N$ interactions at N^2LO involve two LECs which govern the strength of the one-pion-exchange-contact term and purely contact $3N$ interaction contributions. Conventionally, these LECs are expressed in terms of two dimensionless parameters c_D and c_E. We follow the common practice [6, 30–32] and use the ^{3}H binding energy as one of the observables to provide a correlation between c_D and c_E.

A wide range of observables has been considered in the literature to constrain the remaining LEC. In Ref. [12] different ways to fix this LEC in the 3-nucleon sector were explored, and it was shown that it can be reliably determined from the minimum in the differential cross section in elastic nucleon-deuteron scattering at intermediate energies. This allows us to make parameter-free calculations for $A \geq 4$ nuclei. Here, we present results obtained with the LENPIC interaction having a semi-local coordinate space regulator with $R = 1.0$ fm. With this regulator, the LEC values for the $3N$ interactions at N^2LO are $c_D = 7.2$ and $c_E = -0.671$, as determined in Ref. [12]. Application of these interactions to nucleon-deuteron scattering can be found in Refs. [10, 11] for NN-only potentials, along with selected properties of light- and medium-mass nuclei, and in Ref. [12] including the $3N$ interactions at N^2LO.

In order to reduce extrapolation uncertainties by achieving energies of nuclear states closer to convergence in NCSM calculations, we have elected to employ the LENPIC $NN + 3N$ interaction that has been processed through Similarity Renormalization Group (SRG) evolution [33–35] to a scale of $\alpha = 0.08$ fm^4 which corresponds to $\lambda = 1.88$ fm^{-1}. This LENPIC $NN + 3N$ interaction is employed in Ref. [12] and the sensitivity of the NCSM results (i. e. without extrapolation) to α are shown to be reasonably small for selected nuclear properties including ground state (gs) energies. Sensitivity of NCFC energies for 25 p-shell states to α with the same LENPIC $NN + 3N$ interaction is investigated in Ref. [21] and shown to be comparable to or less than the extrapolation uncertainties for this value of the SRG evolution parameter.

This SRG evolution provides a significant reduction in the strong off-diagonal couplings in momentum space of the NN interaction while, at the same time, inducing contributions to the $3N$ interaction. It is primarily these reductions in couplings to higher momentum states that facilitate convergence in the NCSM calculations which then lead to reduced uncertainties in the NCFC results.

2.3 Daejeon16 *NN* potential

Our second choice is a pure NN interaction, Daejeon16 [13], without the addition of a $3N$ interaction. Daejeon16 was developed from an initial χEFT NN interaction at N^3LO [14–16] by SRG evolution to a scale of $\lambda = 1.5$ fm^{-1}.

In addition to SRG evolution, PETs [17–20] were applied so that the resulting Daejeon16 NN interaction provides good descriptions of certain properties of light nuclei. In particular, there are a total of 7 PET parameters chosen to fit estimates of 11 nuclear properties that were obtained in finite basis space NCSM calculations. The estimates of optimal NCSM results were made in anticipation of the corrections that would arise from extrapolation to the full basis limit which would achieve the estimated NCFC results. The selected observables included the binding energies of ^{3}H, ^{4}He, ^{6}Li, ^{8}He, ^{10}B, ^{12}C and ^{16}O. In addition, the PET parameters were chosen to fit the two lowest excited states in ^{6}Li with $(J^\pi, T) = (3^+, 0)$ and $(0^+, 1)$ as well as the first excited $(1^+, 0)$ in ^{10}B and the first excited $(2^+, 0)$ in ^{12}C. Some of these observables have been previously determined to be sensitive to $3N$ interactions, so achieving their accurate descriptions without $3N$ interactions was a significant milestone.

Throughout the SRG and PET processes, the high-quality descriptions of the two-body data are preserved due to the accurate treatment of unitarity at the level of the NN interaction. Of course, the off-shell properties of the NN interactions are modified through these transformations. The PETs that are fitted to properties of light nuclei are attempts to minimize the effects of the neglected $3N$ and higher-body interactions. Of course, this fitting process cannot completely eliminate the effects of these additional interactions and one expects that nuclear observables will be identified that require higher-body interactions for their accurate description.

3 Energies of light nuclei

Here we present our NCFC results for light nuclei from $A = 4$ through $A = 16$. We select results for a total of 22 mostly particle-stable nuclei and include a selection of excited states, both natural and unnatural parity states, that have been experimentally determined to have reasonably narrow widths. Note that we do not anticipate that we can produce NCFC results at the present time that will be as useful for comparing with energies of broad nuclear resonances. Altogether, we report here the energies, spins and parities of a selected set of 74 nuclear states, excluding isobaric analog states. For comparison, we have reported NCFC results on a total of 57(120) states in light nuclei from $A = 6(3)$ through $A = 16$ in Ref. [36] (Ref [37]) with the JISP16 interaction [38], though these JISP16 studies did include several isobaric analog states. These extensive studies with JISP16 employed a variety of extrapolation methods and also included electromagnetic observables. In addition, about half of the states we include here were investigated with the LENPIC interactions in Refs. [12] and/or [21] where the dependence on χEFT truncation order and SRG evolution scale were also investigated.

While we present our theoretical results, along with their uncertainties, in graphical form, it is important to note the limits on the range of $N_{\max}$ values in the NCSM calculations imposed by the available computational resources. These $N_{\max}$ limits depend on whether we employ an $NN + 3N$ interaction or an NN-only interaction [39, 40]. We therefore choose $N_{\max}$ limits based both on the limit of overall available computational resources and on estimates of what is required for reasonably small uncertainties. In Table 1 we list the actual $N_{\max}$ values used for the results presented here.

As mentioned above, we employ a simple three-parameter exponential form to extrapolate the energies to the complete, but infinite-dimensional, basis using a sequence

Table 1: Highest $N_{\max}$ values used in NCSM calculations for NCFC results presented in this work. The numbers in brackets correspond to the highest $N_{\max}$ values for states with unnatural parity.

Nucleus	$3N$ $N_{\max}$	NN $N_{\max}$	Nucleus	$3N$ $N_{\max}$	NN $N_{\max}$
^{4}He	14	20	^{11}Be	8 (9)	11
^{6}He	12	18	^{11}B	8	10
^{6}Li	12	18	^{12}Be	8	10
^{7}Li	12	16	^{12}B	8	10
^{8}He	12	16	^{12}C	8	10
^{8}Li	10	14	^{13}B	8	10
^{8}Be	10	14	^{13}C	8	10
^{9}Li	10	12	^{14}C	8	10
^{9}Be	10 (9)	12 (13)	^{14}N	8	8
^{10}Be	10 (9)	12 (11)	^{15}N	8	8
^{10}B	10 (9)	12 (11)	^{16}O	8	8

of three highest $N_{\max}$ values from Table 1 at fixed basis parameter $\hbar\omega$,

$$E(N_{\max}, \hbar\omega) \approx E_{\infty}(\hbar\omega) + a(\hbar\omega) \exp\left(-b(\hbar\omega) N_{\max}\right). \tag{4}$$

We take as the NCFC extrapolated energy the result at the $\hbar\omega$ that minimizes the amount of extrapolation, $|E(N, \hbar\omega) - E_{\infty}^{N}(\hbar\omega)|$, with N signifying the highest $N_{\max}$ used in that extrapolation, typically at or slightly above the variational minimum in $\hbar\omega$. For an estimate of the extrapolation uncertainty, we take the maximum of the following quantities:

- difference with the previous $N_{\max}$ extrapolation: $|E_{\infty}^{N-2} - E_{\infty}^{N}|$;
- 20% of the extrapolation: $0.2 * |E(N, \hbar\omega) - E_{\infty}^{N}(\hbar\omega)|$;
- half of the variation in the extrapolated value, $0.5 * |\Delta E_{\infty}^{N}(\hbar\omega)|$, over a range in $\hbar\omega$ around the optimal extrapolation; with the range of 7.5 MeV for Daejeon16, and the range of 8 MeV (6 MeV if the extrapolation is at $\hbar\omega = 16$ MeV) for LENPIC.

While more extensive extrapolation studies have been performed [22–27], we have observed that this simple procedure is reasonably accurate for a range of different states and interactions. In addition, our main thrust here is to apply our methods not only to the gs energies but also to the energies of the excited states. In all cases, we will extrapolate the total energy of each state independent of, for example, the gs energy. This already represents a significant undertaking yet still neglects important energy correlation information. We anticipate that more complete extrapolation analyses will be conducted with these same calculated energies in the future and will lead to refined estimates of converged energies and improved uncertainty estimates.

We present in Figs. 1 and 2 the total energies, spins and parities of the gs and selected excited states of nuclei ranging from $A = 4$ through $A = 10$ and from $A = 11$ to $A = 16$, respectively. All of these nuclei are particle-stable, with the exception of

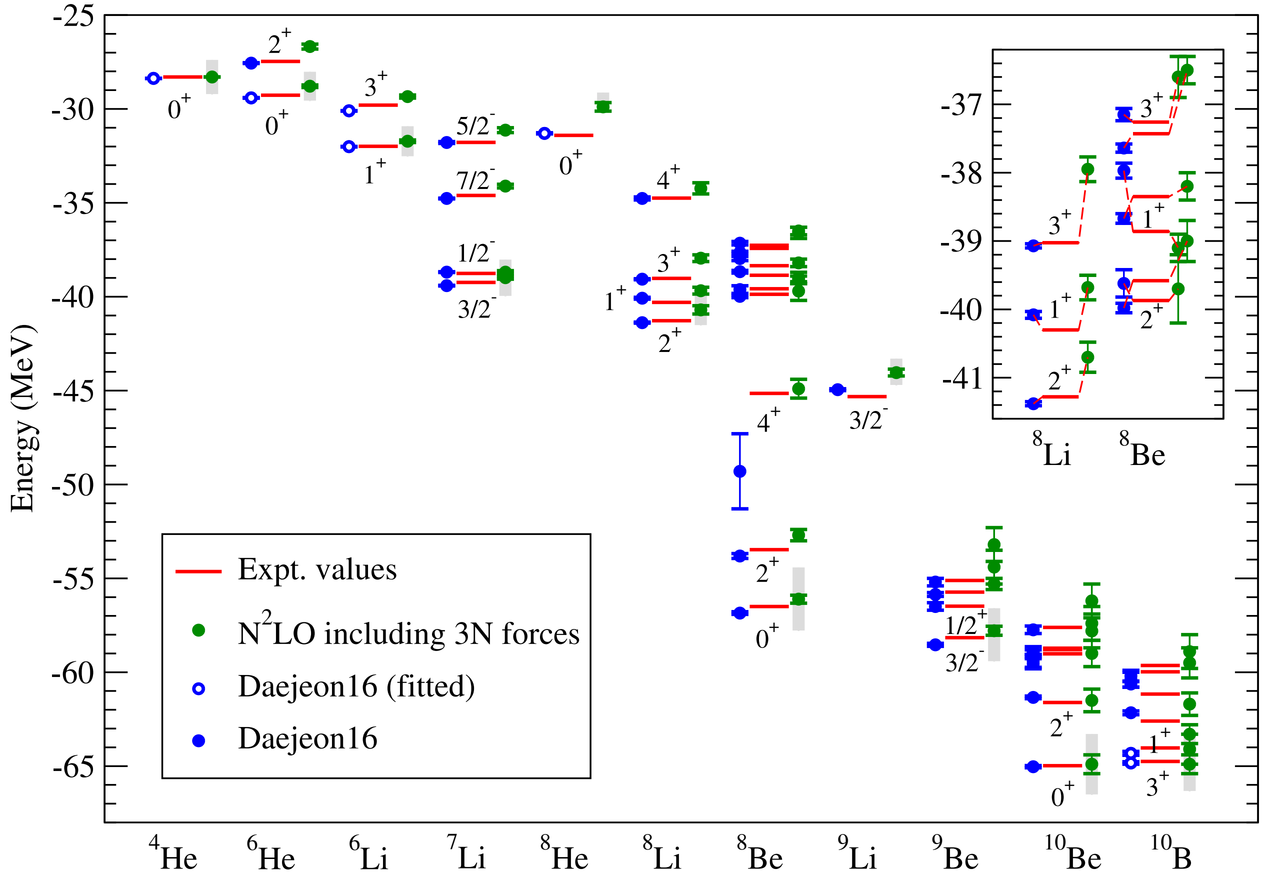

Figure 1: Calculated and experimental energies, spins and parities of the gs and selected excited states of $A = 4$ through $A = 10$ nuclei. States employed to determine PET parameters for Daejeon16 [13] are indicated with open symbols; the grey bands indicate examples of uncertainty from truncation at N^{2}LO in the χEFT expansion [12]. Experimental results are taken from Refs. [41–44].

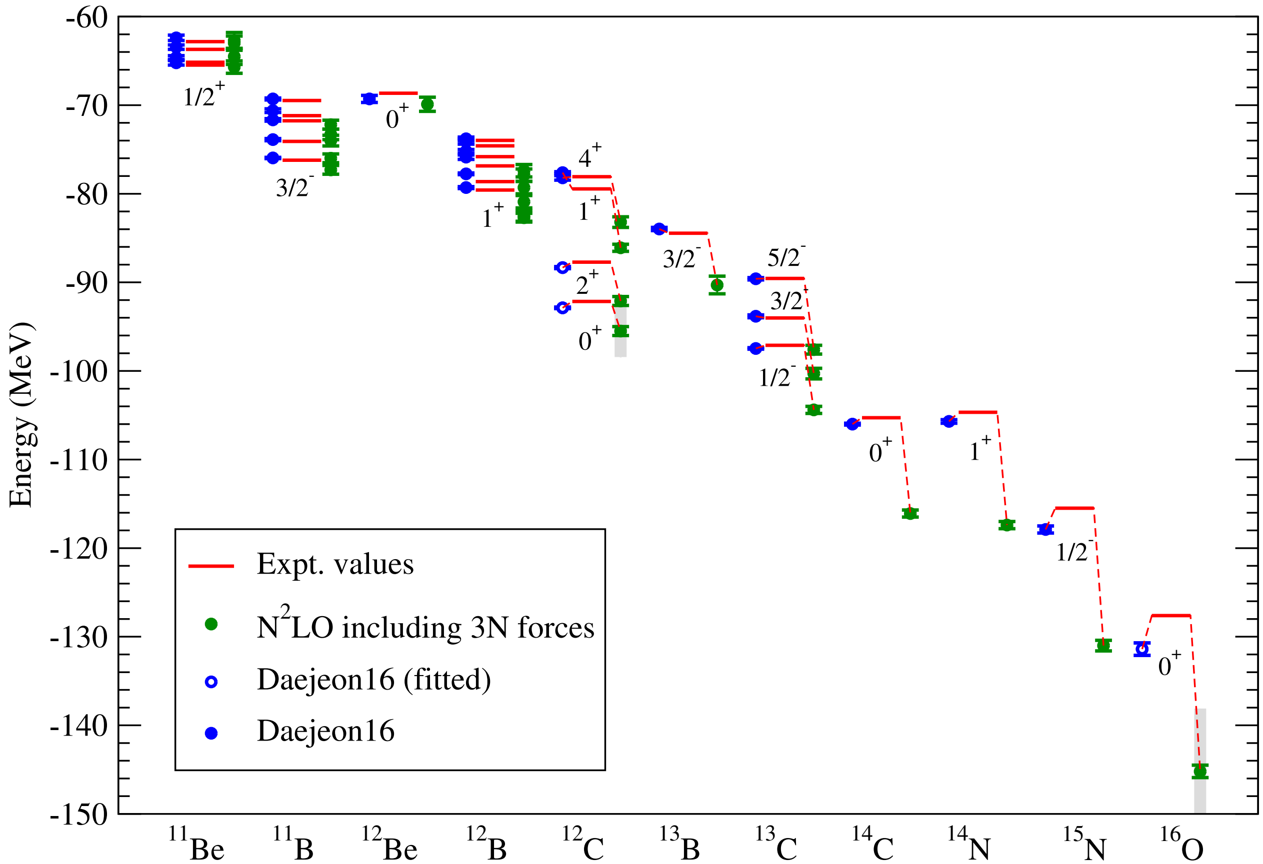

Figure 2: Calculated and experimental energies, spins and parities of the gs and selected excited states of $A = 11$ through $A = 16$ nuclei. States employed to determine PET parameters for Daejeon16 [13] are indicated with open symbols; the grey bands indicate examples of uncertainty from truncation at N^2LO in the χEFT expansion [12]. Experimental results are taken from Refs. [41–44].

^{8}Be; furthermore, all of the excited states shown are narrow, with a width that is less than 300 keV, except for the 2^+ and 4^+ rotational excitations of the gs of ^{8}Be.

For each state, we plot the total experimental energy (sometimes referred to as the total interaction energy), and the NCFC energies for the the Daejeon16 potential and for the complete LENPIC N^{2}LO interaction at $R = 1.0$ fm, SRG evolved to a scale of $\alpha = 0.08$ fm^4. The symbols represent the NCFC result from extrapolation to the complete (infinite-dimensional) basis and the error bars represent the estimated extrapolation uncertainty. States employed to determine PET parameters for Daejeon16 [13] are indicated with open symbols: seven states from $A = 4$ to $A = 10$, two states in ^{12}C, and ^{16}O. The grey bands indicate examples of uncertainty in the gs energies from truncation at N^{2}LO in the χEFT expansion [12]; all of the LECs for the LENPIC interaction were fitted to $A = 2$ and $A = 3$ experimental data. The inset in Fig. 1 presents more detail for selected excited states of ^{8}Li and ^{8}Be.

The first observation from the results in Fig. 1 is the overall good agreement between theory and experiment, within the theoretical uncertainties, for all the states shown. Both interactions give the correct gs spin and parity for all 11 nuclei shown in the lower p-shell. Furthermore, almost all experimental excited states have a corresponding theoretical state with each of the two interactions. The exception is the first excited 0^+ in ^{10}Be: with Daejeon16 we do obtain this state in our calculated low-lying spectrum, but not with the LENPIC N^{2}LO interaction (see Fig. 3 below for more details). More significantly, the level orderings of the theory results are nearly all correct to within extrapolation uncertainties. Exceptions to the correct level ordering occur in the spectrum of ^{8}Be above 15 MeV of excitation, and the cluster of five states in a 300 keV window around 6 MeV excitation energy in ^{10}Be.

Extrapolation uncertainties are considerably smaller for Daejeon16 energies than for the LENPIC $NN+3N$ energies. This difference arises from two sources. The most important source is the difference in the NCSM basis spaces employed where results for LENPIC $NN+3N$ are obtained in smaller basis spaces than the Daejeon16 results (see Table 1) due to the increased computational burden of $3N$ interactions [39, 40]. In addition, the difference in the SRG evolution scales favors the convergence rate for Daejeon16 since Daejeon16 is based on an interaction that has been evolved to a lower momentum scale (1.5 fm^{-1}) compared to the SRG evolution scale of the LENPIC $NN + 3N$ interaction (1.88 fm^{-1}).

Proceeding now to nuclei in the upper half of the p-shell, we see in Fig. 2 that both interactions again give the correct gs spin and parity, with the possible exceptions of the parity inversion in ^{11}Be and the gs of ^{12}B with the LENPIC N^{2}LO interaction. Furthermore, the theoretical level orderings for the low-lying narrow excited states (up to ^{13}C) are again in good agreement with experiment to within extrapolation uncertainties, as shown in more detail below.

However, Fig. 2 also reveals the trend towards overbinding that emerges for the LENPIC N^{2}LO interaction starting at about ^{12}B and for the Daejeon16 interaction at about ^{15}N. It had been established from the beginning that Daejeon16 slightly overbinds ^{12}C by almost 1% and overbinds ^{16}O by about 3.8 MeV [13]. It is also known that the LENPIC N^{2}LO interaction overbinds starting around $A = 12$: for both ^{12}B and ^{12}C this overbinding is only slightly larger than the estimated chiral truncation error, but for ^{16}O the overbinding is significantly more than the chiral truncation error, and the origin of this overbinding is, as yet, unclear [12]. Note however that the LENPIC interaction is entirely fixed by $A = 2$ and $A = 3$ systems,

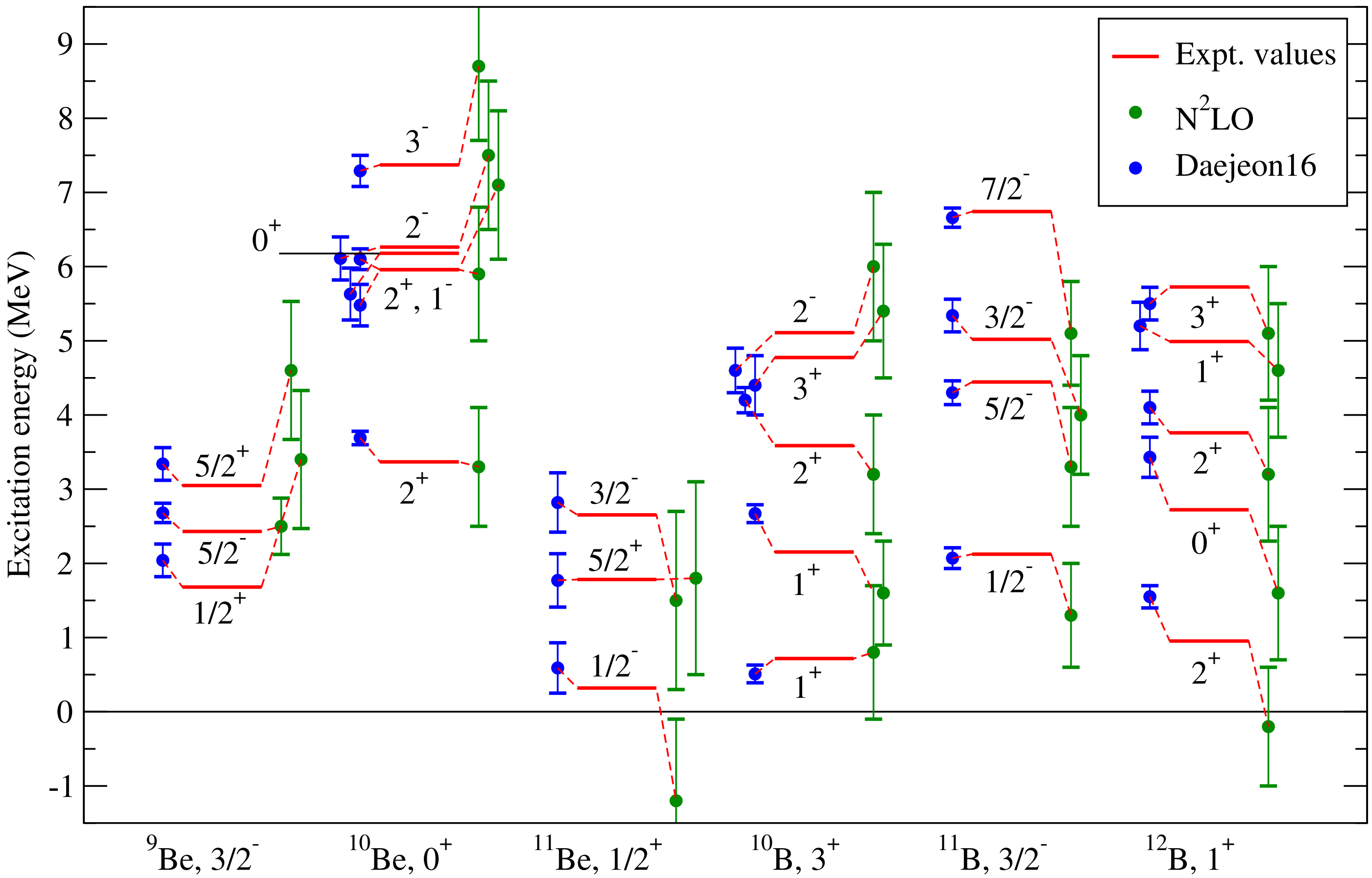

Figure 3: Calculated and experimental excitation energies, spins and parities of selected excited states of six nuclei from $A = 9$ to $A = 12$. Experimental results are taken from Refs. [41–44].

whereas the PET parameters of Daejeon16 were adjusted to fit estimates of p-shell nuclei including ^{12}C and ^{16}O.

In order to examine the low-lying spectroscopy of selected $A = 9$ to $A = 12$ nuclei in more detail and to highlight a few exceptional cases, we present their excitation energies on an expanded scale in Fig. 3. To compare with the experimental excitation energies, we have plotted the difference in the independently extrapolated theoretical total energies and treated the the uncertainties of the extrapolated energy of the gs and the excited state as independent; that is, the shown uncertainty is the root-mean-square sum of the extrapolation uncertainties of the gs and the excited state. This should be a conservative estimate of the uncertainty in the excitation energy since NCSM excitation energies are known to be better converged than the total energies [36].

We note the overall good agreement for most states between theoretical and experimental level orderings in Fig. 3 to within extrapolation uncertainties. Even the appearance of low-lying unnatural parity states in these three nuclei appears well-described with one notable and subtle exception, the gs parity of ^{11}Be with the LENPIC N^{2}LO interaction discussed below. This overall good agreement indicates that these interactions are successfully encapsulating an important aspect of the cross-shell physics which is becoming important for accurately describing intruder states in the low-lying spectra of light nuclei in the mid p-shell region.

The experimental gs spin of ^{10}B has become a celebrated example of the reputed importance of $3N$ interactions in nuclei [31,45]. The conclusion from calculations with realistic NN interactions, but without $3N$ interactions, was, generally, a predicted gs spin of 1^+ with a low-lying excited 3^+ state. However, the experimental information has that order reversed with a 3^+ ground state. The LENPIC $NN + 3N$ interaction at N^{2}LO has already been shown to produce the correct level ordering in ^{10}B [12] concurring with established wisdom since the ordering was found to be incorrect at N^{2}LO without the $3N$ interaction [11].

This conventional wisdom on the critical need for a $3N$ interaction has previously been called into question by the ^{10}B results with Daejeon16 [13] and also by results with JISP16 [37]. However, the extrapolation uncertainties for the JISP16 results left room for doubt that it was the first interaction to serve as a counterpoint to this conventional wisdom. Here, our extrapolation uncertainties are sufficiently small in Fig. 3 that we confirm the results of Ref. [13] showing Daejeon16 does indeed serve as a clear demonstration that subtle $3N$ effects can be accommodated in a realistic NN interaction. This example serves as an important reminder that NN interactions and their $3N$ counterparts are not unique and that unitary transformations can, in principle, transform important properties back and forth between them.

Another celebrated example of subtle effects in light nuclei is the parity inversion experimentally observed in ^{11}Be with a $J^\pi = \frac{1}{2}^+$ gs. This parity inversion has been attributed to the role of continuum physics [46] which is assumed to be absent in calculations, such as ours, retaining the pure HO basis. Contrary to the claim of the need for explicit continuum physics, we find, as shown in Fig. 3 and discussed by Y. Kim at this meeting [47], that Daejeon16 generates the correct parity-inverted gs for ^{11}Be. At the same time, the LENPIC N^{2}LO interaction appears to fail to generate the correct parity-inverted gs. In fact, a closer look at Fig. 3 reveals that all eight (two in ^{9}Be, three in ^{10}Be, two in ^{11}Be, and one in ^{10}B) unnatural-parity states are too high in the spectrum with the LENPIC N^{2}LO interaction, whereas with

Daejeon16 they are significantly closer to the experimental data, and often within the uncertainty estimates.

Less obvious, bot not necessarily less important, is the narrow first excited 0^+ state in ^{10}Be at about 6.2 MeV. With Daejeon16 we do find this state, close to the experimental excitation energy, but with the the LENPIC N^{2}LO interaction we do not find an excited 0^+ state in the low-lying spectrum. It is unclear whether this is due to the more limited basis size with the $3N$ forces, or due to differences in the interactions — to our knowledge, most other interactions, including JISP16, also fail to reproduce this excited 0^+ state in ^{10}Be at the experimental excitation energy.

Finally, let us consider the important case of the lowest two states in ^{12}B. Daejeon16 produces the correct gs spin (1^+) and the first excited state (2^+). However, as noted previously [12], the LENPIC N^{2}LO interaction reverses the ordering of these two states and we reaffirm that conclusion in Fig. 3 while noting that extrapolation uncertainties are significant in this case. We also note that the Daejeon16 results for the low-lying states of ^{12}B all appear to be in good agreement with experiment.

4 Summary and Outlook

We have investigated the spectra of light nuclei from $A = 4$ to $A = 16$ in the NCFC approach with two recent internucleon interactions, the LENPIC $NN + 3N$ interaction and the Daejeon16 NN interaction. We have presented extrapolated energies and their uncertainties for 74 states in 22 nuclei including states of both parities, excluding isobaric analog states. The extrapolation uncertainties are shown to be sufficiently small that the theoretical results are found to be in good agreement with experimental data for most states. Both these interactions overbind nuclei at the upper end of the p-shell which suggests an area for future improvements to the internucleon interactions. Comparing results between Daejeon16 and LENPIC $NN + 3N$ shows the former interaction to have smaller extrapolation uncertainties and to produce somewhat better agreement with experiment, in particular in the upper half of the p-shell. The experimental parity inversion in ^{11}Be and the experimental 1^+ gs spin of ^{12}B provide two examples of subtle effects where the Daejeon16 results agree with experiment while the LENPIC $NN + 3N$ results appear to be deficient. The better performance of the Daejeon16 interaction should not be too surprising since PETs used in its determination were selected to fit a set of properties of light nuclei.

Overall, we find that the extrapolation uncertainties for the spectroscopy of light nuclei with realistic internucleon interactions have been sufficiently reduced in order to make meaningful detailed comparison between theory and experiment and between different internucleon interactions. As our quantum many-body methods continue to improve and the available computational resources continue to increase, we anticipate providing ever more precise diagnostics of state-of-the-art internucleon interactions and increasingly robust predictive power.

Acknowledgments

We thank our collaborators on the co-authored papers cited here for insightful discussions and for providing files of interaction matrix elements used in our previously published works cited herein. This work was supported by the US Department of Energy under Grant Nos. DE-SC0018223 (SciDAC-4/NUCLEI) and DE-FG02-87ER40371, and by the Rare Isotope Science Project of Institute for Basic Science funded by Ministry of Science and ICT and NRF of Korea (2013M7A1A1075764). This research used resources of the National Energy Research Scientific Computing Center (NERSC) and the Argonne Leadership Computing Facility (ALCF), which are US Department of Energy Office of Science user facilities, supported under Contracts No. DE-AC02-05CH11231 and No. DE-AC02-06CH11357, and computing resources provided under the INCITE award 'Nuclear Structure and Nuclear Reactions' from the US Department of Energy, Office of Advanced Scientific Computing Research.

References

[1] P. Maris, J. P. Vary and A. M. Shirokov, Phys. Rev. C **79**, 014308 (2009).

[2] P. Navrátil, J. P. Vary and B. R. Barrett, Phys. Rev. Lett. **84**, 5728 (2000).

[3] B. R. Barrett, P. Navrátil and J. P. Vary, Prog. Part. Nucl. Phys. **69**, 131 (2013).

[4] http://www.lenpic.org.

[5] S. Weinberg, Phys. Lett. B **251**, 288 (1990).

[6] E. Epelbaum, A. Nogga, W. Gloeckle, H. Kamada, U.-G. Meißner and H. Witala, Phys. Rev. C **66**, 064001 (2002).

[7] E. Epelbaum, H. W. Hammer and U.-G. Meißner, Rev. Mod. Phys. **81**, 1773 (2009).

[8] E. Epelbaum, H. Krebs and U.-G. Meißner, Eur. Phys. J. A **51**, 53 (2015).

[9] E. Epelbaum, H. Krebs and U.-G. Meißner, Phys. Rev. Lett. **115**, 122301 (2015).

[10] S. Binder *et al.* (LENPIC Collaboration), Phys. Rev. C **93**, 044002 (2016).

[11] S. Binder *et al.* (LENPIC Collaboration), Phys. Rev. C **98**, 014002 (2018).

[12] E. Epelbaum *et al.* (LENPIC Collaboration), Phys. Rev. C **99**, 024313 (2019).

[13] A. M. Shirokov, I. J. Shin, Y. Kim, M. Sosonkina, P. Maris and J. P. Vary, Phys. Lett. B **761**, 87 (2016).

[14] D. R. Entem and R. Machleidt, Phys. Lett. B **524**, 93 (2002).

[15] D. R. Entem and R. Machleidt, Phys. Rev. C **68**, 041001 (2003).

[16] R. Machleidt and D. R. Entem, Phys. Rep. **503**, 1 (2011).

[17] Yu. A. Lurie and A. M. Shirokov, Izv. Ross. Akad. Nauk, Ser. Fiz. **61**, 2121 (1997) [Bull. Rus. Acad. Sci., Phys. Ser. **61**, 1665 (1997)].

[18] Y. A. Lurie and A. M. Shirokov, Ann. Phys. (NY) **312**, 284 (2004).

[19] A. M. Shirokov, A. I. Mazur, S. A. Zaytsev, J. P. Vary and T. A. Weber, Phys. Rev. C **70**, 044005 (2004).

[20] Yu. A. Lurie and A. M. Shirokov, in *The J-matrix method. Developments and applications,* eds. A. D. Alhaidari, E. J. Heller, H. A. Yamani and M. S. Abdelmonem. Springer, 2008, p. 183.

[21] P. Maris, *Ab initio calculations of p-shell nuclei up to N^2LO in chiral Effective Field Theory, to be published in Proc. XLI Brazilian Meeting on Nucl. Phys., 2–6 September 2018, Maresias, SP, Brazil*; arXiv:1906.03703 [nucl-th] (2019).

[22] S. A. Coon, M. I. Avetian, M. K. G. Kruse, U. van Kolck, P. Maris and J. P. Vary, Phys. Rev. C **86**, 054002 (2012).

[23] R. J. Furnstahl, G. Hagen and T. Papenbrock, Phys. Rev. C **86**, 031301 (2012).

[24] S. N. More, A. Ekström, R. J. Furnstahl, G. Hagen and T. Papenbrock, Phys. Rev. C **87**, 044326 (2013).

[25] K. A. Wendt, C. Forssén, T. Papenbrock and D. Sääf, Phys. Rev. C **91**, 061301 (2015).

[26] I. J. Shin, Y. Kim, P. Maris, J. P. Vary, C. Forssén, J. Rotureau and N. Michel, J. Phys. G **44**, 075103 (2017).

[27] G. A. Negoita *et al.*, Phys. Rev. C **99**, 054308 (2019).

[28] H. M. Aktulga, C. Yang, E. G. Ng, P. Maris and J. P. Vary, Concurrency Computat.: Pract. Exper. **26**, 2631 (2014).

[29] M. Shao, H. M. Aktulga, C. Yang, E. G. Ng, P. Maris and J. P. Vary, Comput. Phys. Commun. **222**, 1 (2018).

[30] A. Nogga, P. Navrátil, B. R. Barrett and J. P. Vary, Phys. Rev. C **73**, 064002 (2006).

[31] P. Navrátil, V. G. Gueorguiev, J. P. Vary, W. E. Ormand and A. Nogga, Phys. Rev. Lett. **99**, 042501 (2007).

[32] D. Gazit, S. Quaglioni and P. Navrátil, Phys. Rev. Lett. **103**, 102502 (2009); Erratum: *ibid.* **122**, 029901 (2019).

[33] S. K. Bogner, R. J. Furnstahl and R. J. Perry, Phys. Rev. C **75**, 061001 (2007).

[34] S. K. Bogner, R. J. Furnstahl, P. Maris, R. J. Perry, A. Schwenk and J. P. Vary, Nucl. Phys. A **801**, 21 (2008).

[35] S. K. Bogner, R. J. Furnstahl and A. Schwenk, Prog. Part. Nucl. Phys. **65**, 94 (2010).

[36] P. Maris and J. P. Vary, Int. J. Mod. Phys. E **22**, 1330016 (2013).

[37] A. M. Shirokov, V. A. Kulikov, P. Maris and J. P. Vary, in *NN and 3N interactions*, eds. L. D. Blokhintsev and I. I. Strakovsky. Nova Science, Hauppauge, NY, 2014, p. 231, https://novapublishers.com/shop/nn-and-3n-interactions/.

[38] A. M. Shirokov, J. P. Vary, A. I. Mazur and T. A. Weber, Phys. Lett. B **644**, 33 (2007).

[39] J. P. Vary, P. Maris, E. Ng, C. Yang and M. Sosonkina, J. Phys. Conf. Ser. **180**, 012083 (2009).

[40] P. Maris, M. Sosonkina, J. P. Vary, E. G. Ng and C. Yang, Proc. Comput. Sci. **1**, 97 (2010).

[41] D. R. Tilley, C. M. Cheves, J. L. Godwin, G. M. Hale, H. M. Hofmann, J. H. Kelley, C. G. Sheu and H. R. Weller, Nucl. Phys. A **708**, 3 (2002).

[42] G. Audi, A. H. Wapstra and C. Thibault, Nucl. Phys. A **729**, 337 (2002).

[43] D. R. Tilley, J. H. Kelley, J. L. Godwin, D. J. Millener, J. E. Purcell, C. G. Sheu and H. R. Weller, Nucl. Phys. A **745**, 155 (2004).

[44] J. H. Kelley, J. E. Purcell and C. G. Sheu, Nucl. Phys. A **968**, 71 (2017).

[45] E. D. Jurgenson, P. Maris, R. J. Furnstahl, P. Navrátil, W. E. Ormand and J. P. Vary, Phys. Rev. C **87**, 054312 (2013).

[46] A. Calci, P. Navrátil, R. Roth, J. Dohet-Eraly, S. Quaglioni and G. Hupin, Phys. Rev. Lett. **117**, 242501 (2016).

[47] Y. Kim, I. J. Shin, A. M. Shirokov, M. Sosonkina, P. Maris and J. P. Vary, *see these Proceedings*, p. 15, http://www.ntse.khb.ru/files/uploads/2018/proceedings/Kim.pdf.